LAUNCH DETECTION SATELLITE SYSTEM ENGINEERING ERROR ANALYSIS

M. R. Beaulieu & K. T. Alfriend
Space Systems Academic Group
Naval Postgraduate School
Monterey, CA 93943

T. Jerardi
Johns Hopkins Applied Physics Laboratory
Laurel, MD 20723-6099

Abstract

An orbiting detector of Infrared (IR) energy may be used to detect the rocket plumes generated by ballistic missiles during the powered segment of their trajectory. By measuring angular directions of the detections over several observations, the trajectory properties, launch location, and impact area may be estimated using a nonlinear least-squares iteration procedure. Observations from two or more sensors may be combined to form stereoscopic lines-of-sight (LOS) increasing the accuracy of the algorithm. Presented in this paper is a computer model of an estimation algorithm which determines what parameter, or combination of parameters, will have a significant effect on the error of the tactical parameter estimation. This model, which is coded in MATLAB™, generates observation data and then, using the data, produces an estimate of the tactical parameters, i.e., the time, position, and heading at launch and burnout, and an impact time and position. The effects of time errors, LOS measurement errors, and satellite position errors on the estimation accuracy, determined using analytical and Monte Carlo simulation techniques, are presented.

Introduction

The TRW-built Defense Support Program (DSP) satellites have been the spaceborne segment of NORAD's Tactical Warning and Attack Assessment system since the early 1970's. Using infrared detectors that sense the heat from missile plumes against the Earth background, these orbiting sentries detect ballistic missile launches. The DSP system provides near real time detection information in support of DOD's tactical warning and attack assessment mission, and is supported by a network of fixed and mobile ground stations that process and disseminate information to military commanders worldwide. The Cold War mission of the DSP system was to detect massive intercontinental ballistic missile (ICBM) attacks. The United States' response to such an attack only required timely and ambiguous warning and missile flight times were much longer than the time required to launch a retaliatory attack. Precise radar tracks could be established with enough time to mitigate effects as much as technology allowed.

The current combat environment demands much more from launch detection satellites. The present threat is from tactical missiles (TBMs), which exhibit much cooler and shorter thrust times, and possibly more depressed trajectories than those exhibited by ICBMs. TBMs can be launched from almost anywhere within a large geographical area of interest, with lofted or depressed trajectories. To attack the launcher and/or employ anti-ballistic missile (ABM) weapons or alert potential victims within the impact zone the tactical parameters must be estimated faster and more accurately than was required for the massive ICBM launch. For budgetary reasons the U.S. is forced to use the existing DSP system to counter the TBM threat into the beginning of the next century[1] until the Space Based Infrared System (SBIRS) is operational. More rapid extraction of more precise information from these existing, technology limited satellites must be accomplished in the interim. Anti-ballistic missile (ABM) systems, such as Patriot or Aegis, may be employed as ABM umbrellas in a tactical area of interest, provided they receive precise and timely cueing from DSP.

This raises the question: "How accurate is the information provided by DSP?" To answer this question an engineering error analysis was performed to determine:

- What are the errors present in the detection system?

- Which errors have the greatest effect upon the accuracy of DSP output information?
- What are the effects of the errors, both individually and collectively, on the estimated launch and impact points?

These questions are addressed in this paper. The algorithm used by the tactical warning system (TALON SHIELD/ALERT) to determine the missile trajectory and predict the launch and impact points is modeled, the various errors are introduced and their effect is determined both analytically (statistically) and numerically by simulation. The results presented in this paper are taken from the Masters thesis of the first author[2].

This paper differs from the earlier work by Danis[3] who considered the estimation of the launch point and trajectory from just two observations. In addition, in this paper the errors in impact time and point are analyzed and the approach is different.

DSP

The DSP[4] system consists of one or more satellites in geosynchronous orbit and one or more ground receiving stations. The DSP satellite is 10 meters long, 7 meters in diameter, and weighs over 2300 kilograms (Fig. 1). Each satellite is spun at six rpm along its longitudinal axis with the telescope pointing toward the Earth so that the sensor scans the Earth. A counter-rotating wheel keeps the system in a nominal zero momentum state. This configuration is sometimes called a "yaw spinner". The IR telescope is tilted from the spin axis, so that the photo-electric cell (PEC) array covers the radius of the Earth. As the satellite rotates, the entire surface of the Earth within the field of view (FOV) is scanned by the IR detector as shown in Figs. 2 and 3.

Detection of IR sources is accomplished with the telescope and PEC array portions of the sensor. The PEC-array of the IR detector is mounted with the nadir end at the center of the rotation of the telescope (Fig. 2). The array contains over 6000 detector cells that are sensitive to energy in the infrared wavelengths. As the PEC array scans the FOV, a cell passing across an IR source will generate a voltage with an amplitude proportional to the signal intensity. This voltage signal is termed an IR return, and is transmitted to ground processing stations after amplification and background filtering. Line of sight of the IR source relative to the satellite is determined from the angle of rotation of the telescope at the time of detection and the cell illuminated.

Error Analysis Algorithm

The quality of the trajectory estimation process is of paramount importance to Tactical Ballistic Missile Defense (TBMD). Real-time knowledge of the launch position allow targeting of the launcher. Cueing for ABM systems, such as Patriot and Aegis, requires timely and accurate trajectory information, which can be propagated from knowledge of the state vector at burnout. Impact time and position is extrapolated from the state vector at burnout, and may be used for warning personnel within the target area. Understanding the algorithms and equations employed in the estimation process is necessary to assess the quality of the estimated parameters.

The detection of a TBM launch is the starting point for any ballistic missile defense. DSP does this by detecting IR radiation emitted by the exhaust plume of a launching missile. With detections by two or more spacecraft (stereo) , triangulation of lines of sight can be used to more accurately estimate the boost-phase trajectory, which is then used to calculate launch position, state vector (position and velocity) at engine burnout, and impact position.

The tactical parameter estimation process is composed of several tasks: Initial estimate of the tactical parameters, nonlinear least-squares estimation (refinement) of the tactical parameters, burn-out time estimation, state vector generation, and impact point calculation. The tactical parameters are:

T_0 = Time of launch

L = Loft

ϕ_0 = Launch point geodetic latitude

λ_0 = Launch point geodetic longitude

h_0 = Launch point height above WGS – 84 ellipsoid

α_0 = Flight trajectory azimuth (true heading)

Observational Data

From the observational data the LOS relative to the satellite is determined. With the attitude

Table 1 Example Observational Data

Index	Time (sec)	S/C ID	Intens	Azimuth (rad)	Elevation (rad)	G.H.A. (rad)	Dec. (rad)	Radius (km)
k	T	S/C	I	β	η	gha	δ	R
1	129.36	1	14.0	4.061854	0.115847	0.174532	0	42164.17
2	130.30	2	23.0	2.427020	0.094741	1.221730	0	42164.17
3	135.44	3	32.0	2.062181	0.142310	1.832595	0	42164.17
4	139.36	1	29.0	4.062497	0.115971	0.174532	0	42164.17
5	140.30	2	29.0	2.427264	0.094753	1.221730	0	42164.17
6	145.44	3	40.0	2.061969	0.142405	1.832595	0	42164.17
7	149.36	1	49.0	4.063552	0.116147	0.174532	0	42164.17
8	150.30	2	60.0	2.427660	0.094746	1.221730	0	42164.17
9	155.44	3	65.0	2.061752	0.142493	1.832595	0	42164.17

data which is included in the telemetry and the satellite position as determined by the Air Force Satellite Control Network (AFSCN) the LOS from the satellite to the IR event in Earth centered coordinates can be determined. Table 1 shows a typical set of observations of a single TBM launch.

The index, k, runs from 1 to n, the total number of observations, and is used as a subscript for the remaining symbols to denote a particular observation. Time, T_k, is the time of observation in seconds measured from midnight of the day of the observation. Spacecraft Identification, S/C, identifies which satellite is making the observation. In this example the event was detected by three satellites. The intensity, I_k, is the radiant intensity of the IR return, and is used to select the type of TBM being detected. Azimuth angle, β_k, is the azimuth LOS of the IR return measured clockwise from true south, and has a range of $(0,2\pi)$ radians (Fig. 4). Elevation angle, η_k, is the elevation of the return measured from nadir and has values between (0, 0.175) radians or (0,10) degrees. The satellite position is given in spherical coordinates (Fig. 5). Greenwich hour angle, gha_k, is the angle between the satellite's nadir point and the prime meridian measured east. Declination angle, δ_k, is the angle above or below the equator measured positive north. Radius, R_k, is the distance from the satellite to the Earth's center, measured in kilometers.

TBM Profile

A TBM profile is a description of the nominal powered flight trajectory of a given TBM. A profile consists of IR intensity and the nominal (maximum range) vertical and horizontal ranges from the launch point as a function of time. The detected radiant intensity is compared to TBM profiles in a data base, and the best match is selected as the type of TBM being observed. This selection process is complex and will be assumed to have been done correctly in this study. The downrange and altitude profiles are represented by fourth order polynomials in time of the form:

$$d_p = a_0 + a_1 t + a_2 t^2 + a_3 t^3 + a_4 t^4, \quad \text{downrange}$$
$$h_p = b_0 + b_1 t + b_2 t^2 + b_3 t^3 + b_4 t^4, \quad \text{altitude} \qquad (1)$$

where t is the time of flight from launch and the a_i and b_i are coefficients. These coefficients are not determined by the algorithm, but are assumed to be known from the typing process, i.e., perfect a priori knowledge of the particular observed TBMs nominal trajectory. Since real-life TBMs do not fly the trajectory exactly using the profile introduces an error. This error is ignored in this analysis since the purpose here is to determine the effects of other error sources.

A loft parameter, L, is used to account for trajectories above or below the nominal profile. The actual range and altitude are modeled by

$$d = (1 - 1.5L)d_p$$
$$h = (1 + L)h_p \qquad (2)$$

The loft varies over ± 0.25, $L > 0$ represents a lofted trajectory and $L < 0$ represents a depressed trajectory.

Nonlinear Least Squares Estimation

For the estimation process it is convenient to express the "polar" focal plane observations (β, η) into focal plane "Cartesian" coordinates (u, v) so that the coordinates have similar behavior with respect to errors and noise. The transformation is

$$\begin{aligned} u &= -\tan\eta \sin\beta \\ v &= -\tan\eta \cos\beta \end{aligned} \tag{3}$$

For the nonlinear least squares estimation let $\mathbf{y}$ be the vector of observations, and let $\mathbf{X}$ be the tactical parameter vector, that is

$$\begin{aligned} \mathbf{y}^T &= (y_1, y_2, \ldots, y_n),\ y_k^T = (u_k, v_k) \\ \mathbf{x}^T &= (T_0, L, \phi_0, \lambda_0, h_0, \alpha_0) \end{aligned} \tag{4}$$

Note that vectors are represented by bold face letters. $\mathbf{y_O}$ will represent the actual observations and $\mathbf{y}_C$ the calculated observations based on specific values of the tactical parameters. The nonlinear least squares proceeds as follows: Assume some initial values of the tactical parameters, $\mathbf{x_C}$, (how to obtain these will be discussed later) expand the equations for the observations in a Taylor series about these initial values, and retain the first term of the series.

$$\begin{aligned} \mathbf{y}_O(\mathbf{x}, t) &= \mathbf{y}(\mathbf{x_C}, t) + \left.\frac{\partial \mathbf{y}}{\partial \mathbf{x}}\right|_{\mathbf{x}=\mathbf{x_C}} (\mathbf{x} - \mathbf{x_C}) \\ \mathbf{y}_O(\mathbf{x}, t) &= \mathbf{y_C} + \mathbf{A}\delta\mathbf{x} \\ \mathbf{A} &= \left.\frac{\partial \mathbf{y}}{\partial \mathbf{x}}\right|_{\mathbf{x}=\mathbf{x_C}} \end{aligned} \tag{5}$$

$\mathbf{A}$ is the partial derivative of the observations with respect to the tactical parameters. In the least squares approach we find the values of the tactical parameters, $\mathbf{X}$, that minimize the difference between the calculated observations, $\mathbf{y}_C$, and the actual observations, $\mathbf{y_O}$. That is, we minimize

$$\begin{aligned} Q &= (\mathbf{y_O} - \mathbf{y_C})^{\mathbf{T}} \mathbf{W} (\mathbf{y_O} - \mathbf{y_C}) \\ Q &= (\delta\mathbf{y} - \mathbf{A}\delta\mathbf{x})^{\mathbf{T}} \mathbf{W} (\delta\mathbf{y} - \mathbf{A}\delta\mathbf{x}) \\ \delta\mathbf{y} &= (\mathbf{y_O} - \mathbf{y_C}) \end{aligned} \tag{6}$$

where $\mathbf{W}$ is a weight matrix and is usually taken as a diagonal matrix where the diagonal terms are in the inverse of the variances of the observations. In this analysis we have assumed $\mathbf{W}$ is the identity matrix. We now want to find the change in the value of the tactical parameters, $\delta\mathbf{x}$, that will minimize Q. This is accomplished by taking the partial derivative and setting it equal to zero.

$$\frac{\partial Q}{\partial \delta\mathbf{x}} = 2\mathbf{A}^{\mathbf{T}} \mathbf{W} (\delta\mathbf{y} - \mathbf{A}\delta\mathbf{x}) = 0 \tag{7}$$

If there are n observations then this is a set of 2n equations with six unknowns. The solution is

$$\delta\mathbf{x} = \left(\mathbf{A}^{\mathbf{T}} \mathbf{W} \mathbf{A}\right)^{-1} \mathbf{A}^{\mathbf{T}} \mathbf{W} \mathbf{dy} \tag{8}$$

The process is shown in Figure 6. With an initial estimate of $\mathbf{X}$, calculate the observations $\mathbf{y}_C$ and the matrix of partials $\mathbf{A}$, then with $\delta\mathbf{y} = \mathbf{y_O} - \mathbf{y_C}$ calculate $\delta\mathbf{x}$. (The initial estimate and $\mathbf{A}$ are addressed in the following two sections.) With $(\mathbf{x_C})_j = (\mathbf{x_C})_{j-1} + \delta\mathbf{x}$ continue the process until the changes in $\delta\mathbf{x}$ become smaller than some tolerance. The resulting solution is the best estimate in the least squares sense.

If $\mathbf{W}$ is the inverse of the covariance of the measurement errors then it can be shown that the matrix

$$\mathbf{C} = \left(\mathbf{A}^{\mathbf{T}} \mathbf{W} \mathbf{A}\right)^{-1} \tag{9}$$

is the covariance matrix of the tactical parameters.

Initial Estimate

The initial guess of the launch point is obtained by projecting the LOS for the first observation for each of the satellites detecting the launch onto the surface of the Earth which yields a latitude and longitude. These values are then averaged to obtain the initial guess. For example, if the first three observations are from

different satellites and ϕ_i and $\lambda_i, i=1,2,3$, are the latitudes and longitudes of the projections of the observations onto the surface of the Earth, then the initial estimates are

$$\begin{aligned}\phi_0^{(0)} &= (\phi_1+\phi_2+\phi_3)/3 \\ \lambda_0^{(0)} &= (\lambda_1+\lambda_2+\lambda_3)/3\end{aligned} \tag{10}$$

The initial estimates for L and h_0 are $L=0, h_0=0$. The time of launch is taken as 20 seconds before the first observation, i.e.,

$$T_0 = T_1 - 20 \tag{11}$$

To obtain the heading the last observations from each of the satellites are averaged in the same manner as the first to obtain

$$\begin{aligned}\phi_{last} &= (\phi_{n-2}+\phi_{n-1}+\phi_n)/3 \\ \lambda_{last} &= (\lambda_{n-2}+\lambda_{n-1}+\lambda_n)/3\end{aligned} \tag{12}$$

The heading is obtained from the great circle arc between these two points,

$$\alpha_0^{(0)} = \frac{\pi}{2} - \tan^{-1}\left(\frac{\left(\lambda_{last}-\lambda_0^{(0)}\right)\cos\phi_0^{(0)}}{\left(\phi_{last}-\phi_0^{(0)}\right)}\right) \tag{13}$$

Matrix of Partials

The matrix of partials is best developed by decomposing it into a set of matrix multiplications. Referring to Figure 5 the (X,Y,Z) coordinate is fixed to the Earth and has its origin at the Earth's center. The (U,E,N) coordinate system has its origin at the DSP satellite making the observation and the directions of the coordinates are as shown. Defining

$$\begin{aligned}\mathbf{s} &= (\phi,\lambda,h)^T \\ \mathbf{r} &= (x,y,z)^T \\ \mathbf{w} &= (U,E,N)^T\end{aligned} \tag{14}$$

$$\begin{aligned}\mathbf{A}_1 &= \frac{\partial \mathbf{s}}{\partial \mathbf{x}}, \mathbf{A}_2 = \frac{\partial \mathbf{r}}{\partial \mathbf{s}} \\ \mathbf{A}_3 &= \frac{\partial \mathbf{w}}{\partial \mathbf{r}}, \mathbf{A}_4 = \frac{\partial \mathbf{y}}{\partial \mathbf{w}}\end{aligned} \tag{15}$$

$$\mathbf{A} = \mathbf{A}_4\mathbf{A}_3\mathbf{A}_2\mathbf{A}_1 \tag{16}$$

$\mathbf{A}_4$ is the transformation of the observations from the focal plane into the satellite Cartesian frame, $\mathbf{A}_3$ then transforms them into the Earth centered Cartesian frame and $\mathbf{A}_2$ transforms them into Earth centered spherical coordinates. $\mathbf{A}_1$ is the matrix of partial derivatives of the spherical coordinates with respect to the tactical parameters. This decomposes $\mathbf{A}$ into four matrices which are relatively easy to derive analytically. They are given in the Appendix. The reader is referred to Ref. 2 for their derivation.

Burnout Time Estimation

The estimation of burnout time is based on the TBM profile maximum burn time $(t_{\max})$, the last observation time (T_{last}), and the next potential observation time (T_{next}) had it occurred. The maximum burn time according to the profile is

$$T_{\max} = T_0 + t_{\max} \tag{17}$$

Two cases can occur:

a) If $T_{\max} > T_{next}$ then

$$T_{bo} = T_{last} + (T_{next} - T_{last})/2 \tag{18}$$

b) if $T_{\max} < T_{next}$

$$T_{bo} = T_{last} + (T_{\max} - T_{last})/2 \tag{19}$$

State Vector Generation

The state vector completely defines the TBM's position and velocity. With the tactical parameters and burnout time estimates the altitude and range at burnout are obtained using Eqs. (1) and (2) with

$$t_{bo} = T_{bo} - T_0 \ . \tag{20}$$

Using

$$\theta_{bo} = d_{bo} / R_e \tag{21}$$

where R_e is the Earth radius

$$\phi_{bo} = (\pi/2) - \cos^{-1}\begin{pmatrix}\cos\theta_{bo}\sin\phi_0 + \\ \sin\theta_{bo}\cos\phi_0\cos\alpha_0\end{pmatrix}$$
$$\lambda_{bo} = \lambda_0 + \sin^{-1}(\sin\theta_{bo}\sin\alpha_0/\cos\phi_{bo}) \quad (22)$$
$$alt_{bo} = h_0 + h_{bo}$$

This gives the position, the velocity at burnout is expressed in terms of the speed (V_{bo}), the flight path angle (γ_{bo}) and heading α_{bo}:

$$\begin{aligned} V_{bo} &= \sqrt{\dot{d}^2 + \dot{h}^2} \\ \gamma_{bo} &= \tan^{-1}(\dot{h}/\dot{d}) \\ \alpha_{bo} &= \sin^{-1}(\cos\phi_0\sin\alpha_0/\cos\phi_{bo}) \\ \dot{d} &= \partial d/\partial t, \dot{h} = \partial h/\partial t \end{aligned} \quad (23)$$

The state vector at burnout is $(\phi_{bo}, \lambda_{bo}, h_{bo}, V_{bo}, \gamma_{bo}, \alpha_{bo})^T$.

Impact Position and Time

The ballistic trajectory is modeled in three phases [5]: powered flight, which is the portion DSP observes; free-flight, which is a portion of an elliptic orbit or ballistic trajectory; and re-entry, which is the portion in which atmospheric drag becomes significant until missile impact. The powered flight is modeled with the TBM profile polynomials presented earlier. The ellipse traced during free-flight is simulated using inertial two body mechanics. Atmospheric drag effects during the re-entry phase are not specifically calculated in this model, but are somewhat accounted for by assuming that the distance traveled over the Earth from re-entry to impact is the same as from launch to burnout. This is the same as assuming that the Earth central angles are the same, i.e., $\theta_{re} = \theta_{bo}$. These are approximations, but their effect should be negligible for the error analysis. They would not be negligible if one was concerned with the actual trajectory. See Ref. 2 for details.

Error Sources

Each error source usually has one or more underlying causes. For example, the LOS error is a result of attitude errors and focal plane misalignments. A complete error analysis would break each error source down to its fundamental level, and model each level correctly. In this section, some of the underlying causes of the overall sources are identified, but in these analyses, only the overall error magnitudes are analyzed. The errors are grouped into three types: time, LOS and satellite position. Time errors can be caused simply by having more than one clock referenced as a source of time measurement. Imperfect synchronization between clocks' time and time passage rate are obvious error sources. Time delays caused by radio transmission of data due to distance, atmospheric refraction, and relative motion Doppler effects may add another time error. The magnitude of time errors is relatively small, and getting smaller as time measurements are being made continually.

LOS measurement errors can arise from many sources, primarily attitude uncertainties and IR radiation measurement errors. Any attitude control system inaccuracy effects are amplified by the geosynchronous altitude. The knowledge of the telescope alignment with the satellite's reference frame is defined by the design and manufacturing of the DSP satellite, and changes slightly with thermal variations. The IR radiation measurements of intensity and angle of arrival (AOA) also have several underlying error sources. Locations of the individual photoelectric cells on the focal plane array are recorded in what is termed the "Focal Plane Vector Table" (FPVT). The positions of the PECs change as the satellite heats and cools with varying sun-satellite orientations, causing a warping of the focal plane, but the FPVT does not account for the changes real-time . In addition, detector noise, refraction, and IR attenuation due to clouds and water vapor all add to the total measurement error.

Satellite position measurements from the AFSCN are used to update the ephemeris once per week. The ephemeris is propagated from the time of update to estimate the satellite position for the next week. The measurements are, of course, inexact, and the resulting ephemeris error grows with time during the one week prediction interval.

Since the missile profile, Eqs. (1) and (2), is an approximation of an average trajectory for each missile class it is a source of error. The profiles can be a major error source. However, this analysis does not consider this error source and assumes the profile to be perfect.

Another source of error is the burnout time. This error is not the result of an error in the

system, but is the result of the 10 second scan period. The error in the burnout time is considered in this analysis.

Keeping all these underlying components in mind, the errors are modeled in the tactical parameter algorithm. The real-world error component magnitudes, bias and random distributions may be different from those simulated, but the overall effects manifest themselves in a manner close to the error models. It should be possible to extrapolate the results obtained in this study to different errors by properly scaling the different magnitudes and distributions. It must be emphasized that since the goal of this study is not to exactly determine the tactical parameters at launch, state vector at burnout, or impact time and position. The purpose is to determine the contribution of the various error sources upon these values, and this can be done with approximate models for the errors. If the intended goal is to calibrate the system to eliminate bias errors, then the error sources must be modeled more exactly to determine what is observable.

Results

The algorithm previously described was programmed into MATLAB™. Three error sources, time, satellite position and LOS, were simulated and added to the observational data, first separately, and then combined. The effects of the errors on the results are analyzed at three points: launch position, burnout position, and impact position. Five Middle Eastern Capital cities were chosen as fictitious launch sites to determine the effects of TBM launch position on the accuracy of the results. Except when noted there were three DSP satellites in geostationary orbit at longitudes 10°E, 70°E and 105°E. The approach was Monte Carlo with 1000 runs for each condition.

The model for the time error is a random uniform distribution between zero and one milliseconds. For satellite position, a random normal distribution with zero mean and standard deviation of 200 meters was added to each components, radial, in-track and cross-track. This is approximately a one standard deviation sphere of 346 meters. The LOS error was modeled as a random normal distribution with a standard deviation of five microradians, added to both the β and η components. The values used for the error sources are representative of what can occur.

Figures 7-9 show for a due east launch from Baghdad the distribution and error ellipse for the launch point, burnout point and impact point, respectively. The error ellipse (ellipsoid) is the figure defined by [6]

$$\mathbf{z}^T\mathbf{P}^{-1}\mathbf{z} = 1 \qquad (24)$$

where $\mathbf{z}$ is the vector representing the variables in question, e.g., latitude and longitude, and $\mathbf{P}$ is the covariance matrix for those variables. Recall that the time error and the burnout time are not Gaussian so the covariance matrix does not represent a Gaussian error distribution. Figure 8 is an ellipsoid since the burnout point is three dimensional. Shown in the figure are the three orthogonal ellipses for each set of two axes.

The data for the 300 km TBM were collated by city, heading and error source. The maximum area (volume) of the error ellipse (ellipsoid) obtained from the 1000 runs for each of the three points are shown in Figures 10-18 for each of the three error sources. Figs. 19-21 show the combined error effects for the three points. Each figure has five curves for the five launch points (cities). Immediately apparent is that the launch point has very little effect on the size of the error ellipses and ellipsoids. Also, evident is that the observational geometry and TBM heading have a large effect on the ellipsoid size.

Table 2 summarizes the results by showing the minimum, mean and maximum area (volume) for each error source for the three points. It is evident from the results that the error sources can be ranked in order of effect:

1. LOS errors
2. Satellite position errors
3. Time errors

Taking advantage of the ease of modifying the MATLAB™ code, various changes to the present DSP system model were made to determine the effects upon the accuracy of the results. For these cases the launch site was Baghdad and the observational data were modified by the combined error sources.

The first case is the control case with nominal parameters and is denoted by "Bagcom" to represent "Baghdad combined errors", and is used

Table 2 Error Ellipse Areas and Volumes

Error	Launch Ellipse Area (km^2)			Burnout Ellipsoid Vol (km^2)			Impact Ellipse Area (km^2)		
	min	mean	max	min	mean	max	min	mean	max
time	3.26e-8	2.59e-7	1.22e-6	2.9e-11	3.6e-10	1.33e-9	1.57e-6	2.61e-5	1.41e-4
satpos	3.77e-3	5.27e-3	8.68e-3	6.04e-4	1.14e-3	2.32e-3	6.12e-3	7.92e-3	3.27e-1
LOS	2.97e-2	8.45e-2	1.83e-1	2.37e-2	9.33e-2	2.09e-1	3.05e0	1.02e1	1.95e1
comb.	3.91e-1	1.01e-1	2.97e-1	4.44e-2	1.25e-1	4.50e-1	3.35e0	1.38e1	4.06e1

Table 3 Various Case Comparison

Error	Launch Ellipse Area (km^2)			Burnout Ellipsoid Vol (km^2)			Impact Ellipse Area (km^2)		
	min	mean	max	min	mean	max	min	mean	max
Bagcom	4.21e-2	1.01e-1	2.74e-1	4.46e-2	1.09e-1	2.60e-1	3.83e0	1.40e1	4.04e1
Synchr	4.40e-2	7.07e-2	1.10e-1	2.09e-2	4.89e-2	8.61e-2	3.94e0	7.82e0	1.52e0
Molniya	4.39e-2	7.58e-2	1.25e-1	2.61e-2	5.57e-2	1.04e-1	2.91e0	7.96e0	1.85e1
10 s sc	4.21e-2	1.01e-1	2.74e-1	4.46e-2	1.09e-1	2.60e-1	3.83e0	1.40e1	4.04e1
7.5 s sc	2.62e-2	7.44e-2	1.95e-1	2.53e-2	4.55e-2	1.09e-1	4.03e0	8.72e0	2.08e1
5.0 s sc	2.48e-2	5.02e-2	1.52e-1	1.23e-2	2.52e-2	6.52e-2	2.52e0	5.84e0	1.64e1
2.5 s sc	1.18e-2	2.36e-2	3.48e-2	5.05e-3	9.21e-3	1.31e-2	1.03e0	2.95e0	4.58e0

as a baseline case for comparison. The second case, "Synchr." shows the effect of synchronizing the spins of the satellites so that the satellites scan the area of interest within one second of each other. In the third case, "Molniya", a third satellite at 70°E GHA and 63.4° latitude replaced the DSP satellite at the same longitude to simulate a Molniya + geostationary viewing geometry. The purpose here was to evaluate the effect of better triangulation of the launch. The remaining cases simulated faster scan periods from 10 seconds down to 2.5 seconds. The results are shown in Table 3.

The first two modifications have the effect of decreasing the areas and volume by about 30%. A decrease is expected for the Molniya case since two satellites on the equator and one at high latitude gives better viewing geometry. The synchronized spin results were somewhat of a surprise, however. The effect on the launch ellipse area is fine, but since the burnout time estimate should be less accurate, it would be expected that the burnout ellipsoid volume and impact ellipsoid area would increase. However, they decreased. More research is needed in this area.

Increasing the scan rate has two positive effects; more data is obtained during the boost phase allowing for a better trajectory estimate, and a better estimate of the burnout time is obtained. The decrease in the launch ellipse area and the impact ellipse area are essentially linear with decreasing scan rate and the burnout ellipsoid volume decrease is quadratic.

Conclusions

The TALON SHIELD/ALERT state vector estimation algorithm was modeled in MATLAB™. System errors were modeled and introduced into the algorithm to determine the effects upon accuracy of the final results. The errors were broadly categorized as errors in time, satellite position and LOS. The relative magnitudes of the error effects listed largest to least are:

- LOS - using a zero mean, 5 μradian standard deviation normal error distribution in focal plane coordinates
- Satellite position -using a zero mean, 200 meter standard deviation normal error distribution in satellite position coordinates

- Time - using a uniform error distribution between zero and one millisecond.

As expected, the effects behave independently and the principle of superposition can be used.

References

1. Rodrigues, L. J., Defense Support Program Station Upgrades Not Based on Validated Requirements", *GAO Report to the Acting Secretary of the Air Force*, United States General Accounting Office, May 1993.

2. Beaulieu, M. R., *Launch Detection Satellite System Engineering Error Analysis*, M.S. Thesis, Naval Postgraduate School, March 1996.

3. Danis, N.J., "Space-Based Tactical Ballistic Missile Launch Parameter Estimation," *IEEE Transactions on Aerospace and Electronic Systems*, vol. 29, No. 2, April 1993, pp. 412-424.

4. Bontrager, M. D., "Defense Support Program," *Space Operations Orientation Course Handbook*, Air Force Space Command, 1993, pp. 179-190.

5. Bates, R.R., Mueller,D.D. and White, J.E., *Fundamentals of Astrodynamics*, Dover Publications, Inc., 1971.

6. Torrieri, D.J., "Statistical Theory of Passive Location Systems," *IEEE Transactions on Aerospace and Electronic Systems*, vol. AES-20, No. 2, March 1994, pp. 183-198.

Appendix

In this Appendix the partial derivatives are presented. From Eqs. (4) and (14) - (16)

$$\begin{aligned}
\mathbf{y} &= (u_1, v_1, u_2, v_2, \ldots u_n, v_n)^T \\
\mathbf{x} &= (T_0, L_0, \phi_0, \lambda_0, h_0, \alpha_0)^T \\
\mathbf{s} &= (\phi, \lambda, h)^T \\
\mathbf{r} &= (x, y, z)^T \\
\mathbf{w} &= (U, E, N)^T
\end{aligned} \tag{A1}$$

$$\begin{aligned}
\mathbf{A}_1 &= \frac{\partial \mathbf{s}}{\partial \mathbf{x}}, \mathbf{A}_2 = \frac{\partial \mathbf{r}}{\partial \mathbf{s}} \\
\mathbf{A}_3 &= \frac{\partial \mathbf{w}}{\partial \mathbf{r}}, \mathbf{A}_4 = \frac{\partial \mathbf{y}}{\partial \mathbf{w}}
\end{aligned} \tag{A2}$$

$$\mathbf{A} = \mathbf{A}_4 \mathbf{A}_3 \mathbf{A}_2 \mathbf{A}_1 \tag{A3}$$

$$\mathbf{A}_1^T = \begin{bmatrix}
\frac{\partial d}{\partial T_0}\frac{\cos\alpha_0}{r_{eff}} & \frac{\partial d}{\partial T_0}\frac{\sin\alpha_0}{r_{eff}\cos\phi_0} & \frac{\partial h}{\partial T_0} \\
-\frac{1.5 d_p \cos\alpha_0}{r_{eff}} & -\frac{1.5 d_p \sin\alpha_0}{r_{eff}\cos\phi_0} & h_p \\
1 & 0 & 0 \\
0 & 1 & 0 \\
0 & 0 & 1 \\
-\frac{d\sin\alpha_0}{r_{eff}} & \frac{d\cos\alpha_0}{r_{eff}\cos\phi_0} & 0
\end{bmatrix} \tag{A4}$$

$\mathbf{A}_2$ can be approximated by

$$\mathbf{A}_2 = \begin{pmatrix}
-(r_{eff}+h)\sin\phi\cos\lambda & -(r_{eff}+h)\cos\phi\sin\lambda & \cos\phi\cos \\
-(r_{eff}+h)\sin\phi\sin\lambda & +(r_{eff}+h)\cos\phi\cos\lambda & \cos\phi\sin \\
(r_{eff}+h)\cos\phi & 0 & \sin\phi
\end{pmatrix} \tag{A5}$$

$\mathbf{A}_3$ is the transformation between (XYZ) and (UEN).

$$\mathbf{A}_3 = \begin{pmatrix}
\cos\delta_k & 0 & \sin\delta_k \\
0 & 1 & 0 \\
-\sin\delta_k & 0 & \cos\delta_k
\end{pmatrix} \times \begin{pmatrix}
\cos(gha_k) & \sin(gha_k) & 0 \\
-\sin(gha_k) & \cos(gha_k) & 0 \\
0 & 0 & 1
\end{pmatrix} \tag{A6}$$

From

$$u_k = -\frac{E_k}{U_k}, v_k = -\frac{N_k}{U_k} \tag{A7}$$

$$\mathbf{A}_4 = \begin{pmatrix}
\frac{E_k}{U_k^2} & \frac{-1}{U_k} & 0 \\
\frac{N_k}{U_k^2} & 0 & -\frac{1}{U_k}
\end{pmatrix} \tag{A8}$$

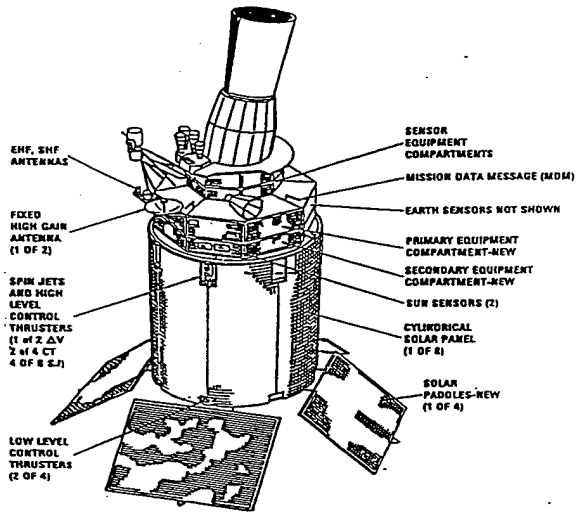

Figure 1 DSP Satellite

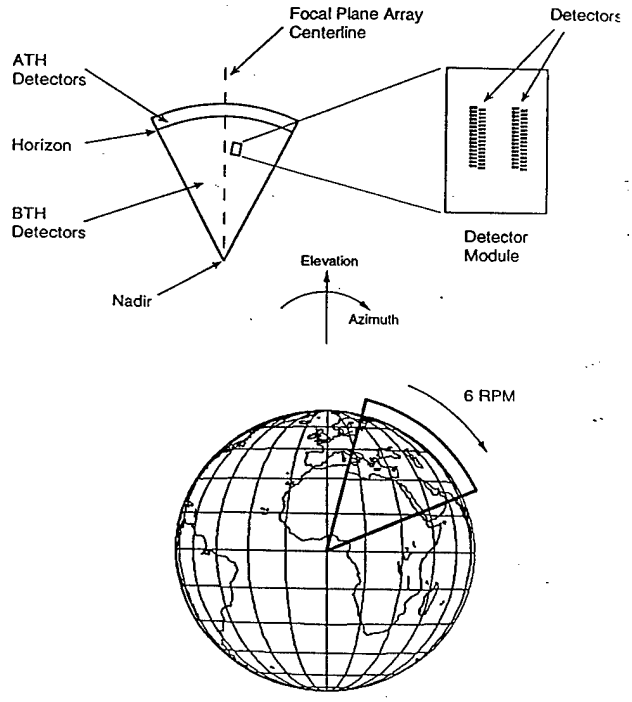

Figure 3 Focal Plane Array Scanning FOV

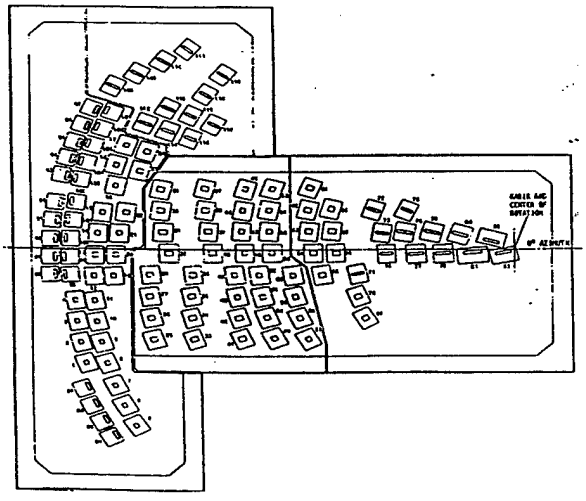

Figure 2 Photoelectric Cell Array

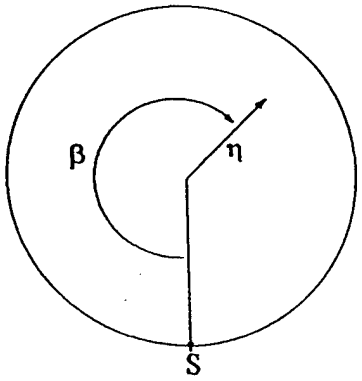

Figure 4 Focal Plane Coordinates

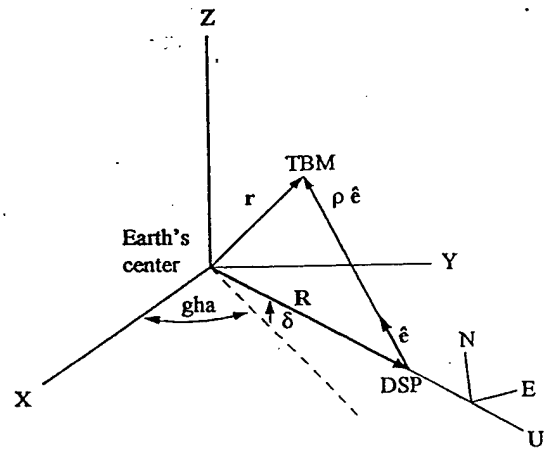

Figure 5 Coordinate Frames

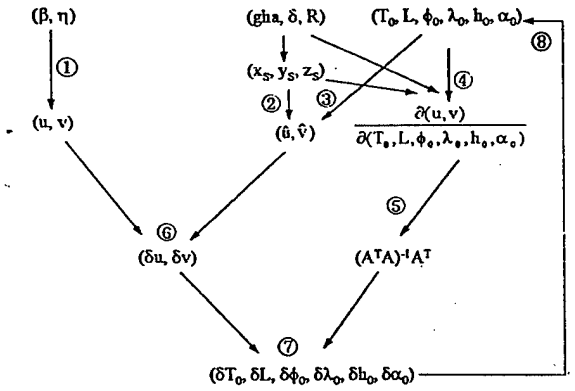

Figure 6 Flowchart Diagram of Iteration Process

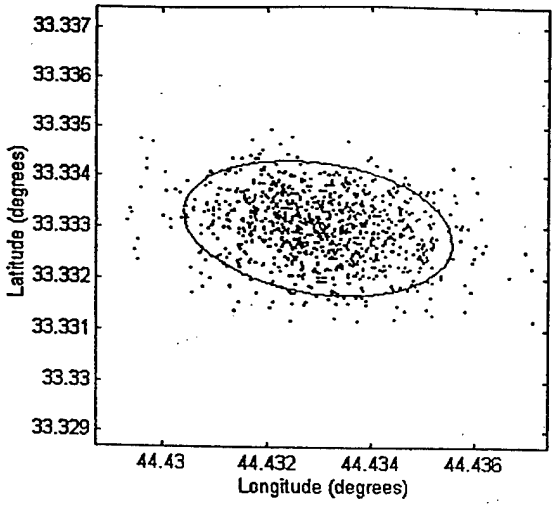

Figure 7 Launch Position Error Ellipse

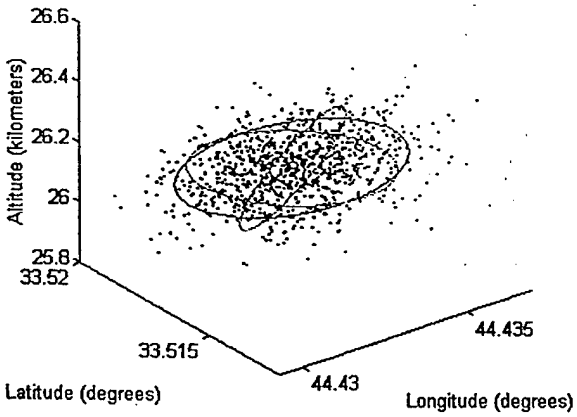

Figure 8 Burnout Position Error Ellipsoid

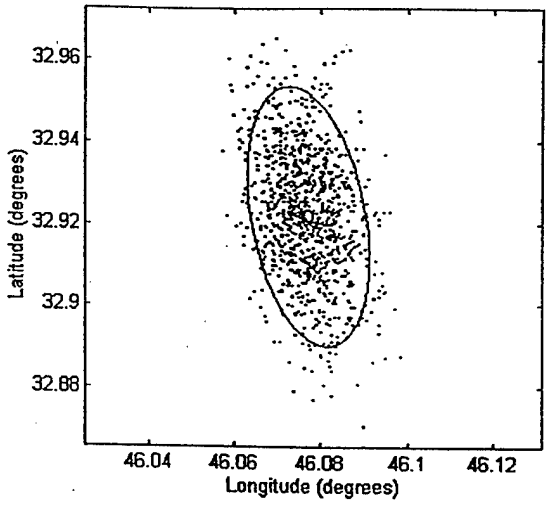

Figure 9 Impact Position Error Ellipse

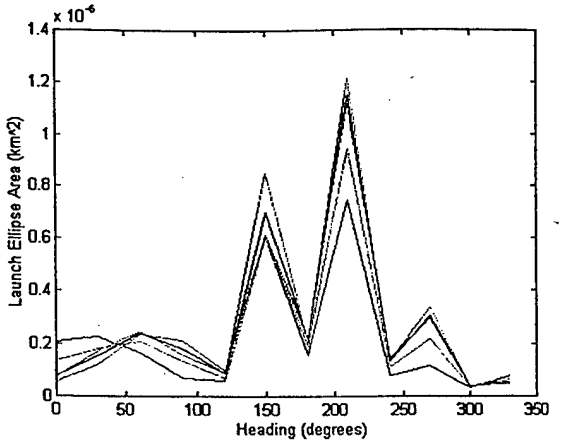

Figure 10 Time Error Effects Upon Launch Ellipse Area

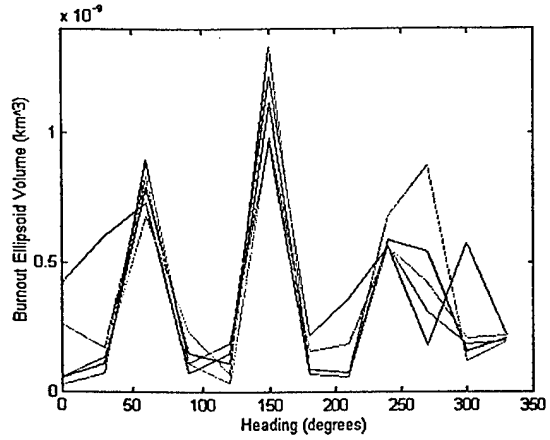

Figure 11 Time Error Effects Upon Burnout Ellipsoid Volume

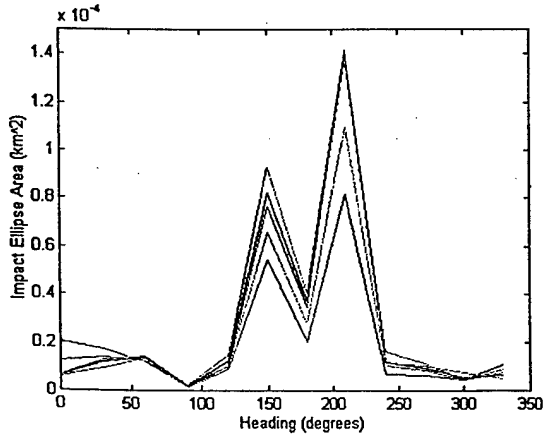

Figure 12 Time Error Effects Upon Impact Ellipse Area

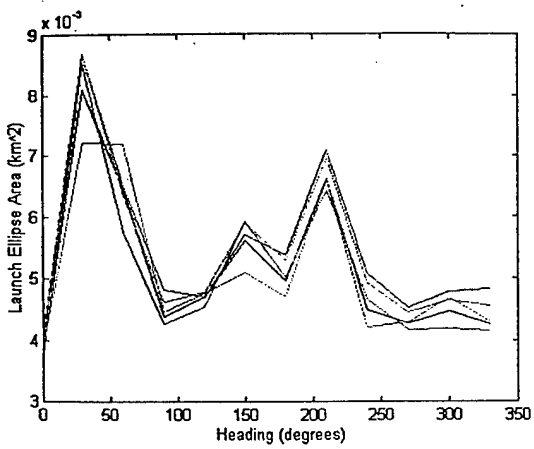

Figure 13 Satellite Position Error Effects Upon Launch Ellipse Area

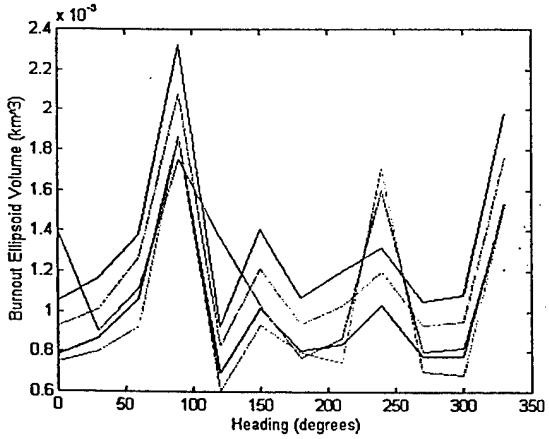

Figure 14 Satellite Position Effects Upon Burnout Ellipsoid Volume

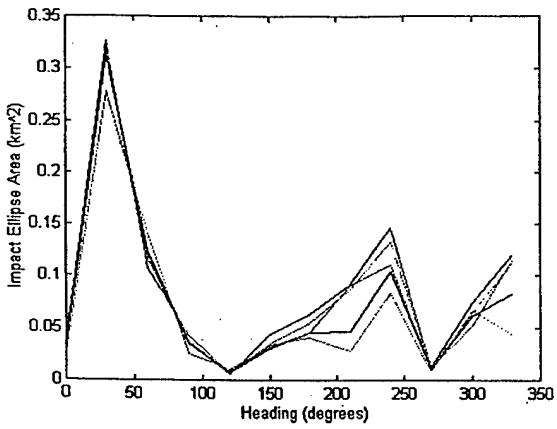

Figure 15 Satellite Position Upon Impact Ellipse Area

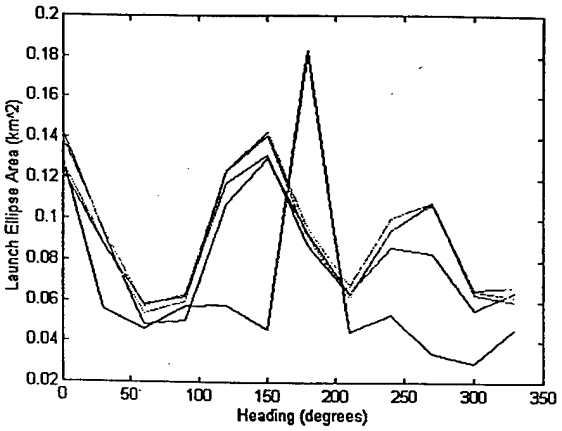

Figure 16 LOS Error Effects Upon Launch Ellipse Area

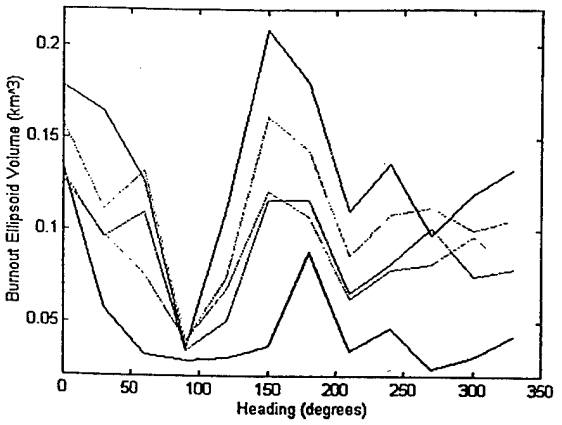

Figure 17 LOS Error Effects Upon Burnout Ellipsoid Volume

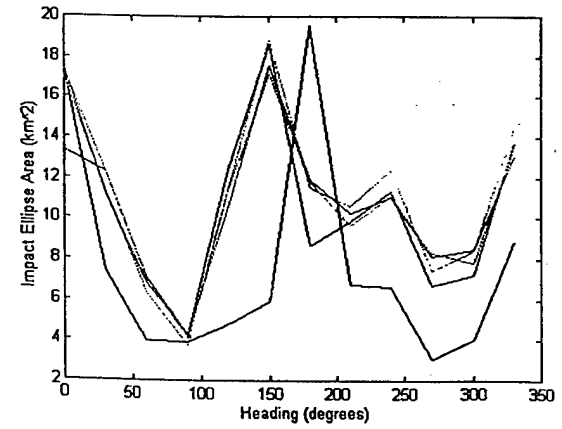

Figure 18 LOS Error Effects Upon Impact Ellipse Area

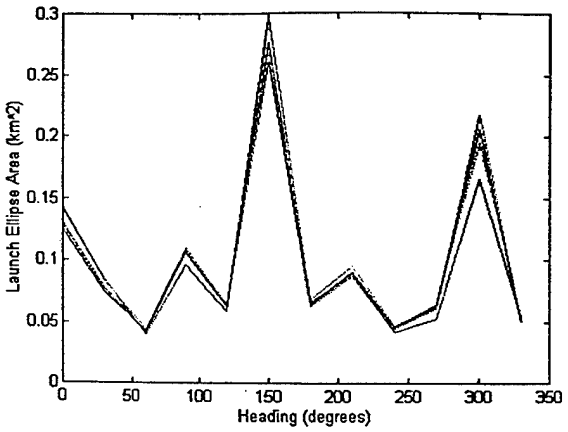

Figure 19 Combined Error Effects Upon Launch Ellipse Area

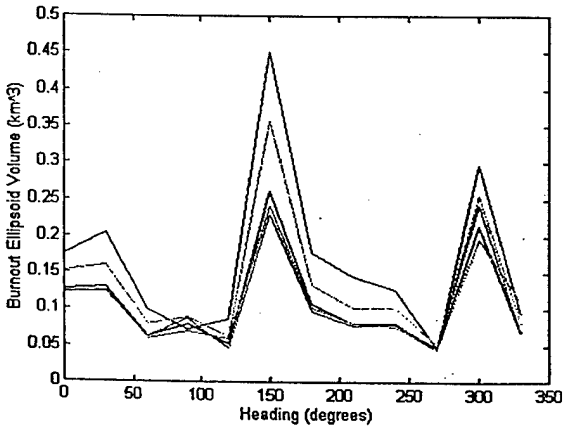

Figure 20 Combined Error Effects Upon Burnout Ellipsoid Volume

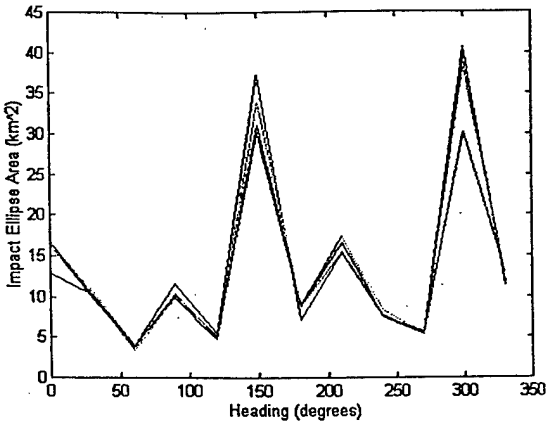

Figure 21 Combined Error Effects Upon Impact Ellipse Area

PLEASE CHECK THE APPROPRIATE BLOCK BELOW: M97-03-2016

☐ _____ copies are being forwarded. Indicate whether Statement A, B, C, D, E, F, or X applies.

☒ DISTRIBUTION STATEMENT A:
APPROVED FOR PUBLIC RELEASE: DISTRIBUTION IS UNLIMITED

☐ DISTRIBUTION STATEMENT B:
DISTRIBUTION AUTHORIZED TO U.S. GOVERNMENT AGENCIES ONLY; (Indicate Reason and Date). OTHER REQUESTS FOR THIS DOCUMENT SHALL BE REFERRED TO (Indicate Controlling DoD Office).

☐ DISTRIBUTION STATEMENT C:
DISTRIBUTION AUTHORIZED TO U.S. GOVERNMENT AGENCIES AND THEIR CONTRACTORS; (Indicate Reason and Date). OTHER REQUESTS FOR THIS DOCUMENT SHALL BE REFERRED TO (Indicate Controlling DoD Office).

☐ DISTRIBUTION STATEMENT D:
DISTRIBUTION AUTHORIZED TO DOD AND U.S. DOD CONTRACTORS ONLY; (Indicate Reason and Date). OTHER REQUESTS SHALL BE REFERRED TO (Indicate Controlling DoD Office).

☐ DISTRIBUTION STATEMENT E:
DISTRIBUTION AUTHORIZED TO DOD COMPONENTS ONLY; (Indicate Reason and Date). OTHER REQUESTS SHALL BE REFERRED TO (Indicate Controlling DoD Office).

☐ DISTRIBUTION STATEMENT F:
FURTHER DISSEMINATION ONLY AS DIRECTED BY (Indicate Controlling DoD Office and Date) or HIGHER DOD AUTHORITY.

☐ DISTRIBUTION STATEMENT X:
DISTRIBUTION AUTHORIZED TO U.S. GOVERNMENT AGENCIES AND PRIVATE INDIVIDUALS OR ENTERPRISES ELIGIBLE TO OBTAIN EXPORT-CONTROLLED TECHNICAL DATA IN ACCORDANCE WITH DOD DIRECTIVE 5230.25, WITHHOLDING OF UNCLASSIFIED TECHNICAL DATA FROM PUBLIC DISCLOSURE, 6 Nov 1984 (Indicate date of determination). CONTROLLING DOD OFFICE IS (Indicate Controlling DoD Office).

☐ This document was previously forwarded to DTIC on _____ (date) and the AD number is _____.

☐ In accordance with the provisions of DoD instructions, the document requested is not supplied because:

☐ It is TOP SECRET.

☐ It is excepted in accordance with DoD instructions pertaining to communications and electronic intelligence.

☐ It is a registered publication.

☐ It is a contract or grant proposal, or an order.

☐ It will be published at a later date. (Enter approximate date, if known.)

☐ Other. (Give Reason.)

_____
Print or Typed Name

_____ _____
Authorized Signature Date Telephone Number

Session 5 #54

Launch Detection Satellite System Engineering & Error Analysis

PLEASE CHECK THE APPROPRIATE BLOCK BELOW:

☐ _____ copies are being forwarded. Indicate whether Statement A, B, C, D, E, F, or X applies.

☒ DISTRIBUTION STATEMENT A:
APPROVED FOR PUBLIC RELEASE: DISTRIBUTION IS UNLIMITED

☐ DISTRIBUTION STATEMENT B:
DISTRIBUTION AUTHORIZED TO U.S. GOVERNMENT AGENCIES ONLY; (Indicate Reason and Date). OTHER REQUESTS FOR THIS DOCUMENT SHALL BE REFERRED TO (Indicate Controlling DoD Office).

☐ DISTRIBUTION STATEMENT C:
DISTRIBUTION AUTHORIZED TO U.S. GOVERNMENT AGENCIES AND THEIR CONTRACTORS; (Indicate Reason and Date). OTHER REQUESTS FOR THIS DOCUMENT SHALL BE REFERRED TO (Indicate Controlling DoD Office).

☐ DISTRIBUTION STATEMENT D:
DISTRIBUTION AUTHORIZED TO DOD AND U.S. DOD CONTRACTORS ONLY; (Indicate Reason and Date). OTHER REQUESTS SHALL BE REFERRED TO (Indicate Controlling DoD Office).

☐ DISTRIBUTION STATEMENT E:
DISTRIBUTION AUTHORIZED TO DOD COMPONENTS ONLY; (Indicate Reason and Date). OTHER REQUESTS SHALL BE REFERRED TO (Indicate Controlling DoD Office).

☐ DISTRIBUTION STATEMENT F:
FURTHER DISSEMINATION ONLY AS DIRECTED BY (Indicate Controlling DoD Office and Date) or HIGHER DOD AUTHORITY.

☐ DISTRIBUTION STATEMENT X:
DISTRIBUTION AUTHORIZED TO U.S. GOVERNMENT AGENCIES AND PRIVATE INDIVIDUALS OR ENTERPRISES ELIGIBLE TO OBTAIN EXPORT-CONTROLLED TECHNICAL DATA IN ACCORDANCE WITH DOD DIRECTIVE 5230.25, WITHHOLDING OF UNCLASSIFIED TECHNICAL DATA FROM PUBLIC DISCLOSURE, 6 Nov 1984 (Indicate date of determination). CONTROLLING DOD OFFICE IS (Indicate Controlling DoD Office).

☐ This document was previously forwarded to DTIC on _____ (date) and the AD number is _____.

☐ In accordance with the provisions of DoD instructions, the document requested is not supplied because:

☐ It is TOP SECRET.

☐ It is excepted in accordance with DoD instructions pertaining to communications and electronic intelligence.

☐ It is a registered publication.

☐ It is a contract or grant proposal, or an order.

☐ It will be published at a later date. (Enter approximate date, if known.)

☐ Other. (Give Reason.)

MARTIN R. BEAULIEU
Print or Typed Name

Martin R Beaulieu LT USN
Authorized Signature Date

510-263-2162 X7191
Telephone Number